

# A Dual-Band Through-the-Wall Imaging Radar Receiver Using a Reconfigurable High-Pass Filter

Duksoo Kim\* · Byungjoon Kim · Sangwook Nam

## Abstract

A dual-band through-the-wall imaging radar receiver for a frequency-modulated continuous-wave radar system was designed and fabricated. The operating frequency bands of the receiver are S-band (2–4 GHz) and X-band (8–12 GHz). If the target is behind a wall, wall-reflected waves are rejected by a reconfigurable  $G_m$ - $C$  high-pass filter. The filter is designed using a high-order admittance synthesis method, and consists of transconductor circuits and capacitors. The cutoff frequency of the filter can be tuned by changing the reference current. The receiver system is fabricated on a printed circuit board using commercial devices. Measurements show 44.3 dB gain and 3.7 dB noise figure for the S-band input, and 58 dB gain and 3.02 dB noise figure for the X-band input. The cutoff frequency of the filter can be tuned from 0.7 MHz to 2.4 MHz.

**Key Words:** Dual-Band Receiver, FMCW Radar System,  $G_m$ - $C$  Filter, Reconfigurable High-Pass Filter, Through-the-Wall Radar.

## I. INTRODUCTION

Imaging radar uses radio waves to generate an image of a distant target. Compared to conventional optical imaging systems, radar-based imaging can detect a target regardless of weather or time of day. Although the resolution of the target image is lower than with optical imaging, radio waves can penetrate objects. Therefore, radar-based imaging is suited to security applications, because the system can detect a target hidden behind an obstacle. This type of radar system can be classified as through-the-wall radar [1–3].

Several through-the-wall imaging systems have been researched; however, these are dedicated to a specific frequency band that determines the characteristics of the system. For example, the S-band (2–4 GHz) is useful for detecting a target in a lossy medium, since the S-band signal has good pen-

etration characteristics. However, it also has the drawback of limited image resolution due to its relatively low frequency. On the other hand, the X-band (8–12 GHz) can achieve finer resolution than the S-band, but the detection range of the target is restricted due to its high loss. Thus, a dual-band imaging system is an attractive alternative, since it can flexibly select a suitable frequency according to the situation [4].

In this paper, an imaging radar receiver is designed as part of a dual-band through-the-wall imaging radar system. This receiver front-end can operate in the S-band or X-band, and has the characteristic of attenuating wall-reflected waves when the target is located behind a wall. To reject unwanted reflected waves, a high-pass filter is designed as a key part of the receiver. The filter has reconfigurable frequency response by changing the transconductance of the circuit. In Section II, the design of the overall imaging radar receiver system is des-

Manuscript received November 9, 2015 ; Revised June 20, 2016 ; Accepted June 25, 2016. (ID No. 20151109-058J)

School of Electrical Engineering and Computer Science, Institute of New Media and Communications, Seoul National University, Seoul, Korea.

\*Corresponding Author: Duksoo Kim (e-mail: dskim@ael.snu.ac.kr)

This is an Open-Access article distributed under the terms of the Creative Commons Attribution Non-Commercial License (<http://creativecommons.org/licenses/by-nc/3.0>) which permits unrestricted non-commercial use, distribution, and reproduction in any medium, provided the original work is properly cited.

© Copyright The Korean Institute of Electromagnetic Engineering and Science. All Rights Reserved.

cribed. Section III presents the implementation of the reconfigurable high-pass filter. Section IV presents measurements obtained from the fabricated receiver system, and Section V concludes the paper.

## II. IMAGING RADAR RECEIVER DESIGN

The proposed receiver system of a through-the-wall imaging radar is shown in Fig. 1. The input frequency bands of the receiver are S-band and X-band. The input signal travels from the antenna, and is amplified by a low-noise amplifier (LNA). The antennas are dedicated to one frequency band, so the RF parts of the receiver are designed for each band separately. A switching device is used to select the frequency band electrically. The amplified signal is applied to a mixer and directly downconverted to the baseband. The mixer has wideband characteristics to handle the dual-band input, and the receiver shares the circuit from the mixer stage to the baseband. The local oscillator (LO) signal of the mixer is a frequency-modulated continuous-wave (FMCW) signal, which comes from the transmitter chirp generator.

In an FMCW imaging radar system, the transmitted wave is reflected from the target and enters the receiver antenna. The time-delayed received signal and the transmitted signal are multiplied in a mixer to produce a baseband beat frequency, which is proportional to the distance from the target [5]. When the target is located behind a wall-like obstacle, the wall-reflected wave appears at a lower frequency than the target-reflected wave. Therefore, the system requires a filter to detect the target on the other side of the wall [1, 6]. Moreover, if there is insufficient isolation between the transmitting and receiving antennas, the transmitted signal directly enters the

receiver and generates a large baseband signal. This directly-coupled signal must be rejected, since the large baseband signal can saturate the receiver circuits. To reject the direct coupling signal and the wall-reflected signal, the filtering characteristics of the receiver become important.

In [1], a bandpass filter is used to reject unwanted signals. However, since the implemented filter has a fixed frequency response, the system operation should be adjusted to the filter specification. The receiver system in [1] employs heterodyne architecture to adjust the intermediate frequency (IF) to the center frequency of the filter. The radar system in [6] uses a bank of bandpass filters for rejecting the unwanted signal, and an appropriate filter block is selected depending on the distance to the wall and the target. Rather than adjusting the system operation to the filter specification or using a bank of filters, this paper proposes a receiver with reconfigurable high-pass filter to reject the unwanted signal.

The proposed filtering topology employs a high-pass filter to reject the direct coupling signal and the wall-reflected signal. The baseband signal of the mixer output passes through the amplifier stage shown in Fig. 2. The amplifier stage applies a second-order high-pass filter to reject the direct coupling signal. The distance between the transmitting antenna and the receiving antenna generates a direct coupling signal at a frequency below 100 kHz. Therefore, the cutoff frequency is set to 100 kHz, and this baseband amplifier also amplifies those signals higher than the cutoff frequency, with a gain of 15 dB.

Even if the direct coupling signal is rejected, the wall-reflected wave remains. Therefore, an additional high-pass filter is necessary to attenuate the wall-reflected wave. This filter should be designed to be able to control its cutoff frequency, since the distance between the radar system and the wall and target can vary.

This additional high-pass filter, with its configurable cutoff frequency, is located after the baseband amplifier stage. The cutoff frequency can be adjusted to attenuate the wall-reflected wave and preserve the target-reflected wave. The output signal of the filter is applied to the baseband buffer circuit in Fig. 1, and the buffered signal becomes the final baseband voltage signal.

The resolution of the dual-band radar system is set to 75 cm for the S-band and 25 cm for the X-band. To achieve this

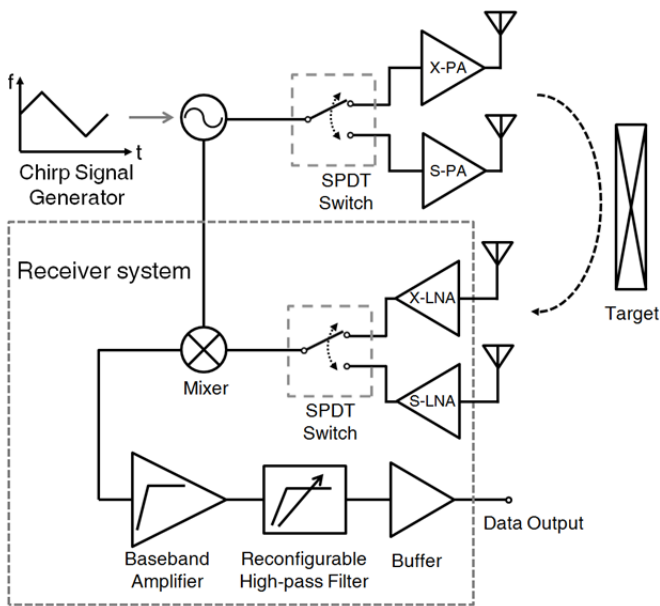


Fig. 1. Block diagram of imaging radar receiver system.

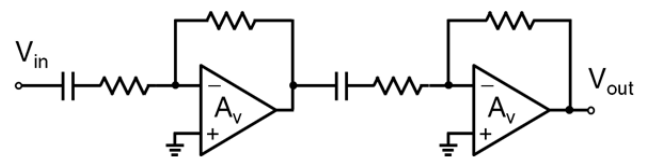


Fig. 2. Block diagram of baseband amplifier stage.

resolution, a transmitting FMCW signal bandwidth of 200 MHz at the S-band and 600 MHz at the X-band are needed, and the receiver has to cover the required bandwidth. The X-band chirp signal generator can be implemented by a digital phase-locked loop (PLL) in [7], which has a chirp signal bandwidth of 600 MHz with center frequency of 9.2 GHz. The S-band chirp signal can be obtained using a divide-by-three circuit at the output of the X-band chirp signal generator. The target range is 3.5 m to 20 m from the radar system. The target detection range sets the cutoff frequency of the high-pass filter, which becomes 0.7 MHz to 2.4 MHz. Since this radar system assumes that the distance from the system to the wall is known, the high-pass filter can be adjusted to appropriate cutoff frequency.

### III. DESIGN OF RECONFIGURABLE HIGH-PASS FILTER

To attenuate the wall-reflected wave, a reconfigurable  $G_m$ - $C$  high-pass filter [8, 9] is designed. A filter of order  $N$  can be synthesized using  $N$  transconductors and  $N$  capacitors.

A high-order admittance synthesis method for high-pass filter formation is illustrated in Fig. 3. With input voltage of  $V_{in}$  and input current of  $I_{in}$ , the admittance  $Y_{in}$  seen from the input becomes

$$Y_{in}(s) = \frac{I_{in}}{V_{in}} = G_{mn} + \frac{G_{m(n-1)}G_{mn}}{sC_n} + \frac{G_{m(n-2)}G_{m(n-1)}G_{mn}}{s^2C_{n-1}C_n} + \dots + \frac{G_{m1}G_{m2} \dots G_{mn}}{s^{n-1}C_2C_3 \dots C_n}. \quad (1)$$

Adding capacitor  $C_1$  to the high-order admittance circuit forms a high-pass filter of order  $N$ . The input voltage is divided into  $C_1$  and  $Y_{in}$ , such that the transfer function of the filter becomes

$$H(s) = \frac{V_{out}}{V_{in}} = \frac{sC_1}{sC_1 + Y_{in}(s)} = \left[ \frac{s^n}{\left( s^n + \frac{G_{mn}}{C_1} s^{n-1} + \frac{G_{m(n-1)}G_{mn}}{C_1C_n} s^{n-2} + \frac{G_{m(n-2)}G_{m(n-1)}G_{mn}}{C_1C_{n-1}C_n} s^{n-3} + \dots + \frac{G_{m1}G_{m2} \dots G_{mn}}{C_1C_2 \dots C_n} \right)} \right]. \quad (2)$$

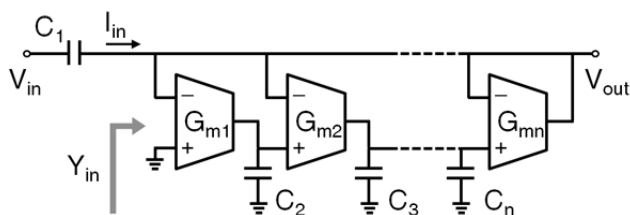


Fig. 3. Block diagram of high-pass filter using high-order admittance synthesis method.

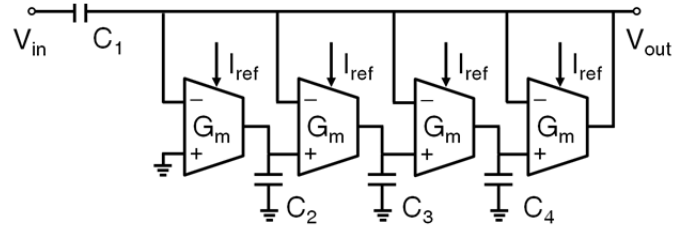


Fig. 4. Block diagram of fourth-order high-pass filter.

A fourth-order high-pass filter (Fig. 4) is designed by Eq. (2). If the transconductor circuits used in the filter have the same transconductance value ( $G_m$ ), the transfer function of the filter is expressed as

$$H(s) = \frac{s^4}{s^4 + c_{41}s^3 + c_{42}s^2 + c_{43}s + c_{44}} \quad (3)$$

where the normalized coefficients of the transfer function are

$$c_{41} = \frac{G_m}{C_1}, c_{42} = \frac{G_m^2}{C_1C_4}, c_{43} = \frac{G_m^3}{C_1C_3C_4}, c_{44} = \frac{G_m^4}{C_1C_2C_3C_4}. \quad (4)$$

Eqs. (3) and (4) show that the frequency response of the high-pass filter can be scaled proportionally by changing the  $G_m$  value. The reconfigurable high-pass filter is designed to have Chebyshev frequency response, and the coefficients of the transfer function are given by  $c_{41} = 0.2756$ ,  $c_{42} = 0.7426$ ,  $c_{43} = 1.4539$ , and  $c_{44} = 0.9528$ . The maximum cutoff frequency of the filter is set to 2.4 MHz. The capacitor values to accomplish the maximum cutoff frequency are  $C_1 = 270$  pF,  $C_2 = 120$  pF,  $C_3 = 39$  pF, and  $C_4 = 27$  pF.

The  $G_m$  values of the transconductors are controlled by a reference current  $I_{ref}$ . Fig. 5 shows the reference current source and a current mirror circuit. The current of the tunable reference current source is duplicated by PMOS transistors. To maintain identical current  $I_{ref}$ , all transistors have the same

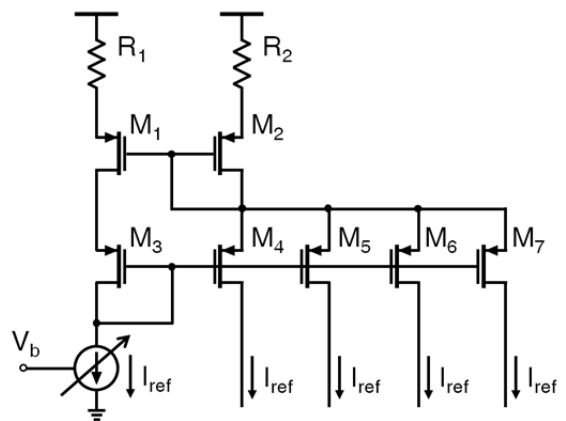


Fig. 5. Block diagram of reference current source and control circuits for transconductors.

width, but transistor  $M_2$  should have a fourfold channel width. The value of the resistor  $R_1$  is four times larger than the resistor  $R_2$  to set the appropriate DC current.

#### IV. MEASUREMENT RESULTS

A dual-band imaging radar receiver was fabricated with reconfigurable high-pass filter. The receiver was implemented on an FR-4 printed circuit board (PCB) and consists of commercial devices. The size of the receiver is  $13.7 \text{ cm} \times 7.5 \text{ cm}$ . Fig. 6 shows a photograph of the receiver. The VDDs for the commercial devices are 3.5 V and 5 V.

The LNAs of each band are cascaded to have appropriate gain at the RF and low noise figure. The X-band LNA is selected to have higher gain than the S-band LNA, since the X-band signal experiences higher loss. A single-pole double-throw switch is used to select the RF input frequency path. The wideband mixer covers the S-band and X-band signals. The baseband amplifier stage in Fig. 2 is implemented, and commercial device OPA211 is used as the operational amplifier. In the reconfigurable high-pass filter, LT1228 devices are used as the transconductors. The reference current source in Fig. 5 is realized by a digital-to-analog converter (DAC) with current output. The transistor  $M_2$  is implemented by a parallel connection of four transistors to have a fourfold channel width.

Frequency responses measured from the receiver are shown in Fig. 7. Single-tone RF and LO signals are applied to the receiver, and the baseband signal at 5 MHz is measured. The S-band shows 44.3 dB gain at 2.8 GHz. In the X-band, gain reaches 58 dB and maintains a flat response over a wide frequency range. In both frequency bands, the desired bandwidths of 200 MHz and 600 MHz are achieved.

Fig. 8 shows the conversion gain and noise figure (NF) measurements by sweeping the baseband frequency. The mi-

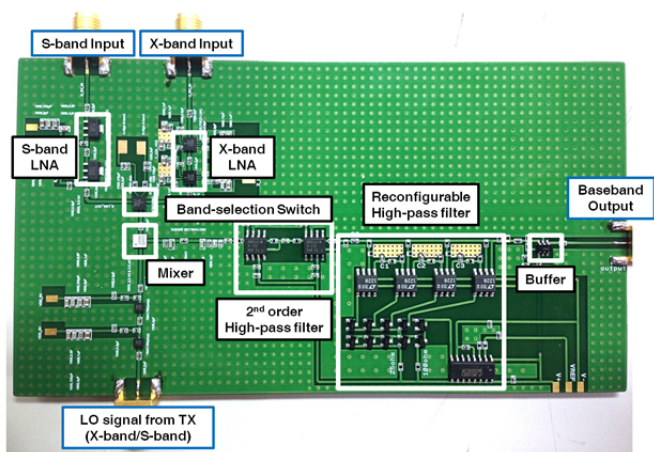


Fig. 6. Photograph of the imaging radar receiver.

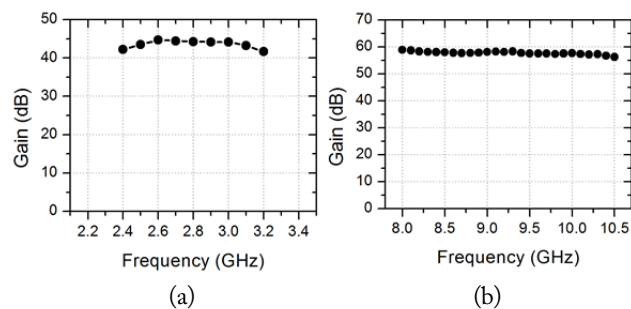


Fig. 7. (a) S-band gain of the receiver. (b) X-band gain of the receiver.

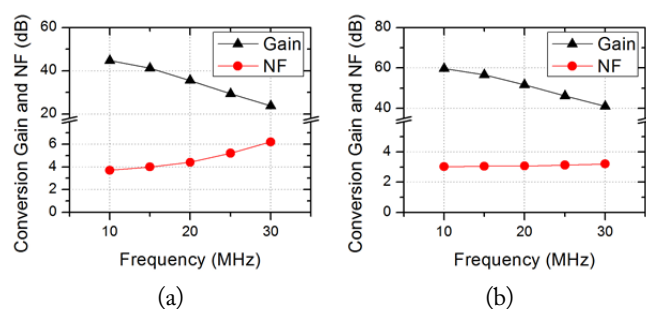


Fig. 8. (a) S-band conversion gain and noise figure (NF) of the receiver. (b) X-band conversion gain and NF of the receiver.

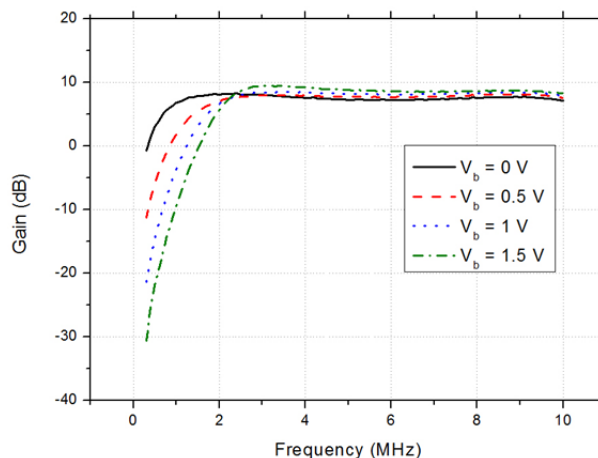


Fig. 9. Frequency response of the reconfigurable high-pass filter.

nimum NFs of the receiver in each band are 3.7 dB and 3.02 dB, respectively.

The frequency response of the reconfigurable high-pass filter part is shown in Fig. 9. The graph shows the change of cutoff frequency with the control of the bias voltage. The cutoff frequency of the filter can be tuned from 0.7 MHz to 2.4 MHz, with bias voltage of 0 V to 2 V.

The location of the target and the wall are assumed for two cases. The first case assumes the wall is located less than 1.5 m away, and the target ranges from 7 m to 20 m. The second case sets the wall's location at 1.5 m to 4 m, and the target from 10 m to 20 m. The filter with bias voltage of 0.5 V corresponds to the first case, and the bias voltage of 1.5 V

corresponds to the second case. In both cases, the attenuation of the wall-reflected wave exceeds 20 dB, compared to the target-reflected wave.

### V. CONCLUSION

A dual-band receiver of a through-the-wall FMCW imaging radar system was designed, and a reconfigurable high-pass filter was implemented as a key part of the receiver. The high-pass filter stage is designed using a high-order admittance synthesis method, and consists of transistor circuits and capacitors.

A reconfigurable high-pass filter-based receiver system was designed, which can operate at S-band and X-band frequencies. The high-pass filter can be tuned to reject wall-reflected waves at low frequencies, enabling effective target detection.

This work was supported by ICT R&D program of MSIP/IITP (No. B0717-16-0045, Cloud based SW platform development for RF design and EM analysis).

### REFERENCES

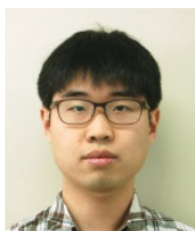
- [1] G. L. Charvat, L.C. Kempel, E. J. Rothwell, C. M. Coleman, and E. L. Mokole, "A through-dielectric radar imaging system," *IEEE Transactions on Antennas and Propagation*, vol. 58, no. 8, pp. 2594–2603, 2010.
- [2] P. H. Chen, M. C. Shastry, C. P. Lai, and R. M. Narayanan, "A portable real-time digital noise radar system for through-the-wall imaging," *IEEE Transactions on Geoscience and Remote Sensing*, vol. 50, no. 10, pp. 4123–4134, 2012.
- [3] J. Laviada, A. Arboleya, F. Lopez-Gayarre, and F. Las-Heras, "Broadband synthetic aperture scanning system for three-dimensional through-the-wall inspection," *IEEE Geoscience and Remote Sensing Letters*, vol. 13, no. 1, pp. 97–101, 2016.
- [4] V. Jain, F. Tzeng, L. Zhou and P. Heydari, "A single-chip dual-band 22–29-GHz/77–81-GHz BiCMOS transceiver for automotive radars," *IEEE Journal of Solid-State Circuits*, vol. 44, no. 12, pp. 3469–3485, 2009.
- [5] M.I. Skolnik, *Introduction to Radar Systems*, 3rd ed. New York: McGraw-Hill, 2001.
- [6] G. L. Charvat, *Small and Short-Range Radar Systems*. New York: CRC Press, 2014.
- [7] S. Ryu, H. Yeo, Y. Lee, S. Son, and J. Kim, "A 9.2 GHz digital phase-locked loop with peaking-free transfer function," *IEEE Journal of Solid-State Circuits*, vol. 49, no. 8, pp. 1773–1784, 2014.
- [8] M. Olsak, L. Matejcek, K. Vrba, and Z. Smekal, "Realization of Nth-order electronically tunable highpass filter employing only N OTAs," in *Proceedings of 10th International Conference on Telecommunications (ICT)*, Tahiti, 2003, pp. 671–676.
- [9] D. Kim, B. Kim, and S. Nam, "A transistor and tunable  $G_m$ -C high-pass filter linearization technique using feed forward  $G_{m3}$  cancelling," *IEEE Transactions on Circuits and Systems II*, vol. 62, no. 11, pp.1058–1062, 2015.

Duksoo Kim



received a B.S. degree in electrical engineering from the Seoul National University, Seoul, Korea, in 2011, and is currently working toward a Ph.D. His main research interests are wideband RF receivers and radar systems.

Byungjoon Kim



received a B.S. degree in electrical engineering from the Seoul National University, Seoul, Korea, in 2009, and is currently working toward a Ph.D. His main research interests are RF components and radar systems.



Sangwook Nam

received a B.S. degree from Seoul National University, Seoul, Korea, in 1981; an M.S. degree from the Korea Advanced Institute of Science and Technology (KAIST), Seoul, Korea, in 1983; and a Ph.D. from The University of Texas at Austin, Austin, TX, USA, in 1989, all in electrical engineering. From 1983 to 1986, he was a researcher with the Gold Star Central Research Laboratory, Seoul, Korea. Since 1990, he has been a Professor at the School of Electrical Engineering and Computer Science, Seoul National University. His research interests include analysis/design of electromagnetic (EM) structures, antennas, and microwave active/passive circuits.